A model for adsorbed monolayers of orientable molecules

1979 J. Phys. C: Solid State Phys. 12 5333

(http://iopscience.iop.org/0022-3719/12/23/036)

J. Phys. C: Solid State Phys., Vol. 12, 1979. Printed in Great Britain.

A model for adsorbed monolayers of orientable molecules

B W Southern† and D A Lavis‡
Institut Laue–Langevin 156X Centre de Tri, 38042 Grenoble Cedex, France

Received 1 May 1979

Abstract. Real-space renormalisation group methods are used to study a two-dimensional lattice fluid model on a triangular lattice with application to adsorbed monolayers of orientable molecules. The phase diagram is obtained for various strengths of the couplings between the molecules. There are four different phases which correspond to the gas, liquid and commensurate solid phases of the model. Two types of solid phase are considered: the first is a close-packed solid phase in which all molecules have the same orientation relative to the substrate and the second is an open honeycomb structure in which the molecules have opposing orientations. The fixed points and critical exponents which describe the transitions between these different phases are obtained. In all cases the melting transition is found to be second order. The results may have some application to monolayers of methane or ammonia, adsorbed onto a graphite substrate.

1. Introduction

The study of two-dimensional models is important because of the increasing experimental investigation of physically and chemically adsorbed systems. Adsorbed monolayers on an ideal substrate may exhibit transitions between 'two-dimensional (2D) gas', '2D liquid' and '2D solid phases' as the substrate coverage is varied (Thomy and Duval 1970). Rare-gas monolayers on graphite have been extensively studied using a variety of experimental methods and transitions from commensurate structures to structures which are incommensurate with the substrate have also been observed (see McTague *et al* 1979 for a recent survey). In the case of the 'commensurable solids', lattice gas models have been employed to describe the melting transition (Schick *et al* 1977, Berker *et al* 1978). The adsorbed molecules are assumed to be well localised on preferred adsorption sites on the substrate and in the case of graphite these sites form a triangular lattice. Since two molecules adsorbed onto nearest-neighbour sites experience an unfavourable potential because of size effects, the registered solid phase in the rare-gas systems corresponds to a preferential occupation of one of the three sublattices of the adsorption site lattice. In contrast, the liquid phase has, on average, equivalent occupation of all three sublattices. In any real system, the solid phase will consist of three different types of domain within which one of the three sublattices is preferentially occupied. These

† Present address: Department of Physics, University of Manitoba, Winnipeg, Manitoba, Canada R3T 2N2.
‡ On leave from: Mathematics Department, Chelsea College, University of London, Manresa Road, London SW3 6LX, UK.

0022-3719/79/235333+11 $01.00

domains will be separated by narrow walls. We, however, shall only consider the behaviour which is characteristic of a single domain.

An extension of the simpler lattice fluid models to the case where the molecules have some 'structure' is considered in the present paper. A related model on a triangular lattice was first introduced (Bell and Lavis 1970) to simulate the strongly directional nature of hydrogen bonding in water and aqueous solutions. In the present model each molecule is assumed to be triangular in shape and to have a restricted number of preferred orientations with respect to the underlying triangular lattice of adsorption sites. The model is a slight generalisation of the Blume–Emery–Griffiths (1971) model which has been used to study both ^{3}He–^{4}He mixtures as well as the competition between dipole and quadrupole ordering in magnets. As a result of the orientational degree of freedom, the model can exhibit two different types of commensurable solid phase. One of these is a close-packed (ferromagnetic) solid in which all molecules have the same orientation relative to the substrate and which appears at densities near monolayer completion. At intermediate coverages, an open honeycomb (antiferromagnetic) solid phase can occur in which two thirds of the sites are preferentially occupied by molecules with opposing orientations.

The model is investigated using a real-space renormalisation group (RSRG) method (for a review see Niemeijer and van Leeuwen 1976). The phase diagram is determined for various choices of the coupling constants as a function of the chemical potential μ and also as a function of the molecular density ρ, since the experiments on adsorbed systems are generally performed at constant coverage. The model is introduced in §2 and the renormalisation group transformation is briefly described. In §3 the results for the phase diagram are presented together with the fixed points and critical exponents which describe the various transitions. Our conclusions are summarised in §4.

2. The model

Each molecule is taken to be triangular in shape and is restricted to point towards any of the six nearest-neighbour sites on a triangular lattice. Hence there are two distinct orientations for a molecule at each adsorption site and these are identified with the spin states $S = \pm 1$ of a spin -1 Ising model as shown in figure 1. A vacant site is represented

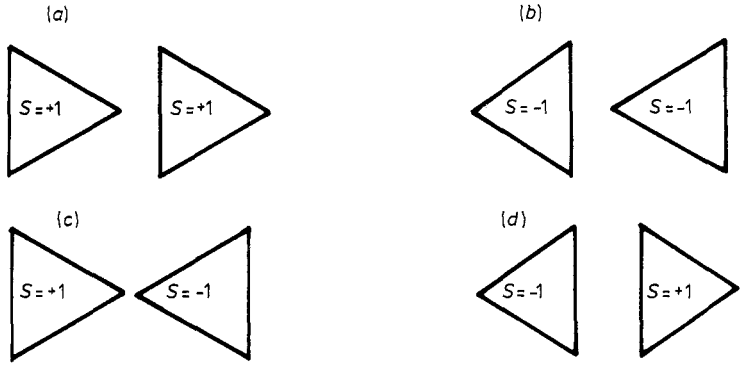

Figure 1. Allowed orientations of a pair of molecules on adjacent sites with the spin states $S = \pm 1$ indicated. Configurations (*a*) and (*b*) have energy $-(\epsilon + \theta)$, (*c*) has energy $-(\epsilon - \theta + w)$ and (*d*) has energy $-(\epsilon - \theta)$.

by the state $S = 0$ and the molecular density is therefore given by $\rho = \langle S_i^2 \rangle$. A pair of molecules on adjacent sites has an energy $-(\epsilon + \theta)$ if they are both in the same orientational state (figure 1*a* and *b*). However, if they have opposite orientations, then there are two possible energies as indicated in figure 1(*c*) and (*d*). Molecules with vertices pointing towards each other have an energy $-(\epsilon - \theta + w)$ whereas molecules with vertices pointing away from each other have an energy $-(\epsilon - \theta)$. The parameter w reflects the difference in separation of the vertices for the pair of molecules in these two cases.

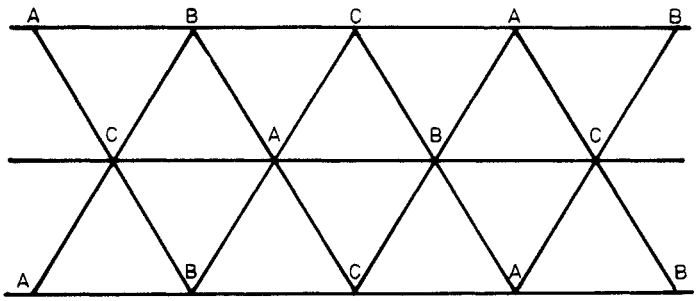

Figure 2. A portion of the triangular lattice showing the convention adopted for labelling the three sublattices A, B and C.

In order to take proper account of sublattice orderings, the triangular lattice is divided into three equivalent sublattices A, B and C as indicated in figure 2. The mean density of molecules is fixed by using the grand canonical distribution with the chemical potential μ as an independent variable. In terms of the spin -1 variables, the Hamiltonian of the system is given by (Young and Lavis 1979)

$$\mathrm{H} = \sum_{\Delta} \mathrm{H}_{\Delta}$$

with

$$H_{\Delta} = -\tfrac{1}{6}\mu(S_{\mathrm{A}}^2 + S_{\mathrm{B}}^2 + S_{\mathrm{C}}^2) - \tfrac{1}{2}(\theta - w/4)(S_{\mathrm{A}}S_{\mathrm{B}} + S_{\mathrm{B}}S_{\mathrm{C}} + S_{\mathrm{C}}S_{\mathrm{A}}) - \tfrac{1}{2}(\epsilon + w/4)(S_{\mathrm{A}}^2S_{\mathrm{B}}^2 + S_{\mathrm{B}}^2S_{\mathrm{C}}^2 + S_{\mathrm{C}}^2S_{\mathrm{A}}^2) + \tfrac{1}{8}w(S_{\mathrm{A}} - S_{\mathrm{B}})(S_{\mathrm{B}} - S_{\mathrm{C}})(S_{\mathrm{C}} - S_{\mathrm{A}}) \quad (1)$$

where the summation is over all elementary triangles of the lattice and $S_{\alpha}(\alpha = \mathrm{A}, \mathrm{B}, \mathrm{C})$ denotes the spin of the site on sublattice α in triangle Δ. Apart from the final term in (1) this Hamiltonian has the same form as the Blume–Emery–Griffiths model. The special feature of the present model is exhibited by the final term which removes the degeneracy associated with cyclic and anticyclic ordering of the states $S = +1, 0, -1$ around an elementary triangle. The model first introduced by Bell and Lavis (1970) corresponds to the case $\theta = 0$.

We use the block spin transformation employed by Schick *et al* (1977) in their study of the spin $-\frac{1}{2}$ Ising model. An initial cluster of nine sites is chosen such that three sites belong to each of the three sublattices and periodic boundary conditions are imposed. Application of the renormalisation group transformation reduces the nine-site cluster to a cluster of three sites, each one belonging to one of the three sublattices, and corresponds to an increase in length scale by a factor of $\sqrt{3}$. In any RSRG calculation all

terms which are generated by the recurrence relations must be included, even if they are not present in the initial Hamiltonian. In our case, two additional terms are generated involving all three spins of the elementary triangles (see Young and Lavis 1979, Southern and Lavis 1980 for details) and we have altogether a six-dimensional space of couplings.

With a suitable choice of relationships between the coupling constants, the full six-dimensional space reduces to a three-dimensional subspace which has the symmetry of an extended three-state Potts model (Young and Lavis 1979). In order to preserve this symmetry we adopt the block spin weight function used by Schick and Griffiths (1977) and Young and Lavis (1979). The conditions for the initial Hamiltonian in equation (1) to lie in this subspace are $\mu = -3(\theta + \epsilon)$ and $w = 3\theta - \epsilon$ and we shall see later that the fixed points in this extended Potts subspace describe the critical behaviour at special points on the phase diagram.

The phase diagram is determined by iterating the recurrence relations for the coupling constant (see Southern and Lavis 1980 for a more detailed discussion). A trajectory which begins at a point where the behaviour of the system is not critical will iterate to a sink which characterises that phase. These regions are separated by the critical regions which form domains of attraction for the critical fixed points. Once these fixed points have been located, the recurrence relations can be linearised about the fixed points and the eigenvalues λ_i of the linear equations can be calculated. The critical exponents y_i are related to the eigenvalues by $\lambda_i = b^{y_i}$, where b is the scale factor and is equal to $\sqrt{3}$ in the present calculation.

3. Phase diagram and critical behaviour

At zero temperature, the behaviour of the model defined in equation (1) can be obtained most easily by comparing the ground-state energies of the seven possible configurations $C_j (j = 1, 2, \ldots, 7)$ of each elementary triangle. The energies $\epsilon_j^{(0)}$ $(j = 1, 2, \ldots, 7)$ of these configurations are given in table 1 in terms of the parameters μ, w, θ, and ϵ. The ground-state phase diagram is shown in figure 3 in terms of the reduced variables $z = (\theta - \epsilon)/(\theta + \epsilon)$, $\tilde{w} = w/(\theta + \epsilon)$ and $\tilde{\mu} = \mu/(\theta + \epsilon)$. In our analysis we have considered only cases for which both $\theta \geqslant 0$ and $\epsilon \geqslant 0$ from which it follows that $-1 \leqslant z \leqslant 1$. Qualitative differences occur in the zero-temperature phase diagrams for negative and positive values of z and these cases are shown in figures 3(*a*) and 3(*b*) respectively.

The only stable ground states are found to be those corresponding to the lattice completely filled by triangles all of which are in one of the configurations C_1, C_2, C_5 or

Table 1. Spectrum of $(-\beta H_\Delta)$.

Configuration C_j	Degeneracy ω_j	Energy ϵ_j^0
C_1 [0, 0, 0]	1	0
C_2 [±1, ±1, ±1]	2	$\beta(\mu + 3\theta + 3\epsilon)/2$
C_3 [0, 0, ±1]	6	$\beta\mu/6$
C_4 [0, ±1, ±1]	6	$\beta(2\mu + 3\theta + 3\epsilon)/6$
C_5 [±1, ∓1, ∓1]	6	$\beta(\mu - \theta + 3\epsilon + w)/2$
C_6 $[+1, 0, -1]_{\text{cyclic}}$	3	$\beta(2\mu - 3\theta + 3\epsilon + 3w)/6$
C_7 $[+1, -1, 0]_{\text{anticyclic}}$	3	$\beta(2\mu - 3\theta + 3\epsilon)/6$

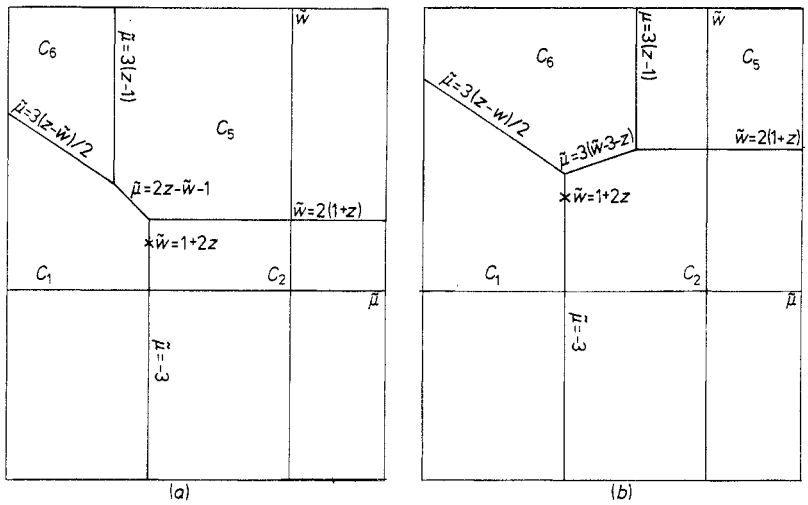

Figure 3. Zero-temperature phase diagram as a function of the reduced variables $\tilde{w} = w/(\theta + \epsilon)$, $\tilde{\mu} = \mu/(\theta + \epsilon)$ and $z = (\theta + \epsilon)/(\theta + \epsilon)$ for (*a*) $-1 \leqslant z \leqslant 0$ and (*b*) $0 \leqslant z \leqslant 1$. In both cases the point which lies in the extended Potts subspace at all temperatures is indicated by a cross.

C_6. The vacant state C_1 corresponds to the gas phase of the model and C_2 is the close-packed (ferromagnetic) solid phase. The close-packed antiferromagnetic state C_5 is highly degenerate with the same ground-state entropy as the spin $-\frac{1}{2}$ Ising antiferromagnet on a triangular lattice and corresponds to the liquid phase of the model (Southern and Lavis 1980). At intermediate values of $\tilde{\mu}$ and $\tilde{w}$, the open honeycomb (antiferromagnetic) structure C_6, which describes a lower-density commensurate solid phase, appears. The domains of these phases at finite temperature are the regions of attraction of the corresponding sinks of the recurrence relations for the renormalised couplings. A numerical study of the trajectory flows allows the construction of the phase diagram in the temperature–chemical potential and temperature–density planes for any initial choice of the parameters z and $\tilde{w}$. Since the aim of this paper is to present a model which exhibits a wide range of possible behaviour rather than to investigate all cases in detail, we have concentrated our attention on the cases $z = \pm 1$ for a number of typical values of $\tilde{w}$. However, we have investigated the fixed point structure for intermediate values of z as well. We find that the case $z = -1$ is typical of all values of z which are negative whereas the case $z = +1$ is a special case for positive values of z. The differences between $z = +1$ and $z < 1$ will be discussed in § 3.3.

3.1. $z = -1$

Our results for the phase diagram in the case $z = -1$ are shown in figures 4(*a*)–(*e*). This case corresponds to the original model introduced by Bell and Lavis (1970) and some of the results for positive values of $\tilde{w}$ have been discussed in the paper by Southern and Lavis (1980). Five basic types of behaviour can occur depending on the value of $\tilde{w}$.

(i) $\tilde{w} < -1$. Figure 4(*a*) shows a typical phase diagram both as a function of the reduced chemical potential $\tilde{\mu} = \mu/\epsilon$ and the molecular number density ρ. The phase

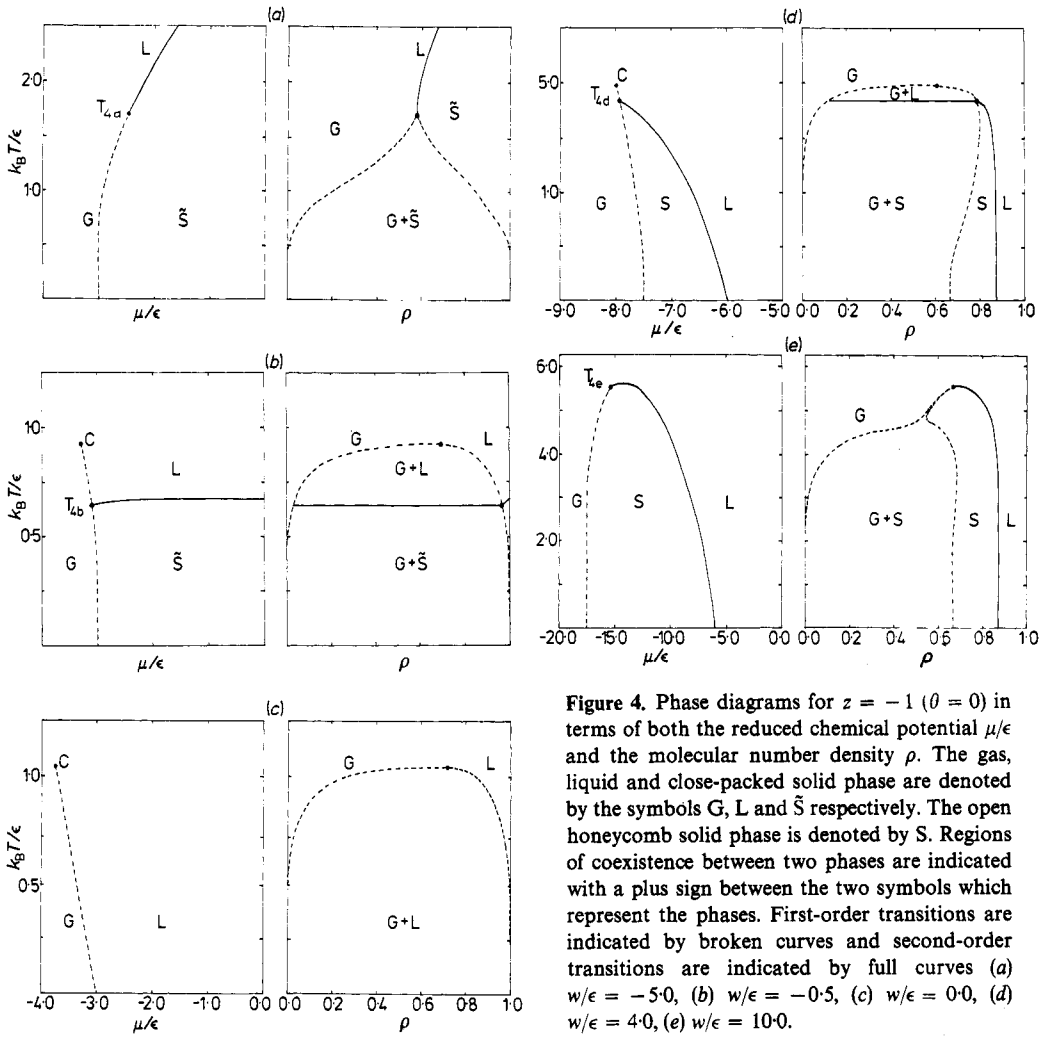

Figure 4. Phase diagrams for $z = -1$ ($\theta = 0$) in terms of both the reduced chemical potential μ/ϵ and the molecular number density ρ. The gas, liquid and close-packed solid phase are denoted by the symbols G, L and $\tilde{S}$ respectively. The open honeycomb solid phase is denoted by S. Regions of coexistence between two phases are indicated with a plus sign between the two symbols which represent the phases. First-order transitions are indicated by broken curves and second-order transitions are indicated by full curves (*a*) $w/\epsilon = -5{\cdot}0$, (*b*) $w/\epsilon = -0{\cdot}5$, (*c*) $w/\epsilon = 0{\cdot}0$, (*d*) $w/\epsilon = 4{\cdot}0$, (*e*) $w/\epsilon = 10{\cdot}0$.

diagram is qualitatively identical to that observed experimentally for monolayers of krypton or nitrogen adsorbed on graphite (Ostlund and Berker 1979). At low temperatures there is a first-order transition (broken curve) between the gas phase (G) and the close-packed solid phase ($\tilde{S}$) while at higher temperatures there is a second-order transition between the liquid phase (L) and $\tilde{S}$. The coordinates and exponents of the fixed points which control these transitions are given in table 2. The first-order transition is described by the discontinuity fixed point G$\tilde{S}$ which has a characteristic relevant exponent $y_1 = d = 2$ (Nienhuis and Nauenberg 1975) and the liquid–solid transition is controlled by the fixed point L$\tilde{S}$ which is identical to the fixed point found by Schick *et al* (1977) for the spin $-\frac{1}{2}$ Ising ferromagnet. These two phase boundaries meet at the tricritical point T_{4a} which lies within the domain of attraction of fixed point N. This latter fixed point is identical to that found by Mahan and Girvin (1978) for the tricritical transition in the ferromagnetic Blume–Capel model (Blume 1966, Capel 1966).

Table 2. Fixed points and critical exponents.

Type	Designation	Location ($x_i = \exp \epsilon_i$)							Exponents					
		x_1	x_2	x_3	x_4	x_5	x_6	x_7	y_1	y_2	y_3	y_4	y_5	y_6
Special multicritical	B^+	1·0	1·000	0·433	0·433	0·433	1·000	0·303	1·901	1·867	1·113	0·282	−0·870	−1·901
Special tricritical	F	1·0	1·000	0·571	0·571	0·571	0·487	0·487	1·608	1·036	0·290	−1·148	−1·583	−1·793
	Z	1·0	0·478	0·376	0·406	0·684	0·938	0·369	1·945	1·097	0·534	−0·683	−1·404	−1·902
Special critical end-line	U	1·0	0·969	0·132	0·319	0·545	0·984	0·194	2·000	1·823	1·018	−0·470	−1·296	−1·988
Tricritical	N	1·0	1·122	0·702	0·675	0·504	0·524	0·524	1·500	0·670	−0·272	−1·058	−1·561	−2·069
	AF^+	1·0	1·000	1·172	1·172	1·172	2·051	1·000	1·036	0·327	−0·983	−1·583	−1·793	−2·124
Critical end-line	V	1·0	0·913	0·000	0·000	0·631	0·000	0·000	2·000	0·638	−0·793	−1·466	−1·466	$-\infty$
	Y	1·0	0·453	0·076	0·213	0·736	0·919	0·171	2·000	1·129	−0·388	−0·388	−1·827	−1·960
Bicritical	M	1·0	21·111	2·653	6·921	11·888	21·435	4·160	1·822	1·017	−0·528	−1·383	−2·067	−3·664
Critical end-point	X	1·0	0·689	0·496	0·515	0·689	0·515	0·515	1·761	0·697	−0·708	−1·151	−1·285	−2·388
First order	GS	1·0	0·000	0·000	0·000	0·000	1·000	0·000	2·000	$-\infty$	$-\infty$	$-\infty$	$-\infty$	$-\infty$
	$G\tilde{S}$	1·0	1·000	0·000	0·000	0·000	0·000	0·000	2·000	$-\infty$	$-\infty$	$-\infty$	$-\infty$	$-\infty$
	$S\tilde{S}$	†0·0	1·000	0·000	0·000	0·000	1·000	0·000	2·000	$-\infty$	$-\infty$	$-\infty$	$-\infty$	$-\infty$
	LG	1·0	0·707	0·000	0·000	0·707	0·000	0·000	2·000	−0·524	−1·052	−1·052	−1·052	$-\infty$
Critical	LS	1·0	20·721	3·373	9·743	33·680	42·017	7·790	1·129	−0·391	−0·391	−1·881	−2·013	−3·687
	$L\tilde{S}$	†0·0	1·000	0·000	0·000	0·691	0·000	0·000	0·638	−0·793	−1·466	−1·466	$-\infty$	$-\infty$

† For these fixed points the maximum x_i has been set equal to one since at least two x_j are infinite on the scale of x_1.

The phase diagram changes qualitatively as $\tilde{w}$ passes through the value $\tilde{w} = -1$. At this value the tricritical point T_{4a} actually lies in the Potts subspace and flows to the fixed point F which was found by Schick and Griffiths (1977) in their study of the ferromagnetic three-state Potts model. In the present model the point T_{4a} plays the role of a special tricritical fixed point.

(ii) $-1 < \tilde{w} < 0$. Figure 4(*b*) shows the type of behaviour which is typical of small negative values of $\tilde{w}$. In addition to the transitions of the previous case, there is now a temperature range below the point C for which a first-order gas–liquid transition occurs. This transition is controlled by the first-order fixed point LG whereas the transition at the critical end–point C itself is described by the fixed point *X*. The liquid–solid, gas–liquid and gas–solid transitions meet at the point T_{4b} which lies in the domain of attraction of fixed point V. This latter fixed point has two relevant exponents and describes the meeting of one critical and two first-order surfaces. The exponents exhibit typical critical end-line behaviour (Berker and Wortis 1976), combining a leading $y_1 = d = 2$ with a $y_2 = 0{\cdot}638$ in close agreement with the leading exponent of LS̃. As $\tilde{w}$ passes through zero we again have a qualitative change in behaviour marked by the complete suppression of the close packed solid phase.

(iii) (iv) (v) $\tilde{w} \geqslant 0$. The results shown in figures 4(*c*)–(*e*) have been discussed previously by Southern and Lavis (1980) in connection with the Bell–Lavis bonding model and will be considered here only briefly. The type of behaviour shown in figure 4(*c*) occurs in the range $0 \leqslant \tilde{w} \leqslant 3$. However, for values of $\tilde{w}$ greater than 3, a second solid phase appears at intermediate densities whose structure has an open honeycomb (antiferromagnetic) arrangement of molecules. The transition between this solid phase (S) and the liquid phase is second-order and controlled by the fixed point LS. The gas–solid and gas–liquid transitions are first-order and described by the first-order fixed points GS and LG respectively. The three phase boundaries intersect at the point T_{4d} which flows to the fixed point Y. For larger values of $\tilde{w}$ the points C and T_{4d} converge until finally the behaviour shown in figure 4(*e*) is attained where the first-order liquid–gas transition has completely disappeared. The gas–solid and liquid–solid phase boundaries meet at the tricritical point T_{4e} which lies in the domain of attraction of the fixed point AF^+. The changeover from the type of behaviour shown in figure 4(*d*) to that shown in 4(*e*) occurs at an intermediate value of $\tilde{w}$ when the domains of attraction of fixed points X, Y and AF^+ intersect. This special point is controlled by the special tricritical fixed point Z. In contrast to the special tricritical fixed point F in §3.1(i) above, Z does not belong to the universality class of the three-state Potts model.

3.2. $z = +1$

Our results for the phase diagram in the case $z = +1$ are shown in figures 5(*a*)–(*c*). This corresponds to the case $\epsilon = 0$ which for $w = 0$ reduces to the Blume–Capel model (Blume 1966, Capel 1966). For $z = +1$, three basic types of behaviour can occur depending on the value of $\tilde{w}$.

(i) $\tilde{w} < 3$. The results shown in figure 5(*a*) are qualitatively the same as those exhibited in figure 4(*a*) and the same fixed points control the various transitions. The change over in behaviour to that shown in figure 5(*b*) occurs at $\tilde{w} = 3$. At this value of $\tilde{w}$ the tricritical point T_{5a} flows to the special multicritical point B^+ which lies in the extended Potts

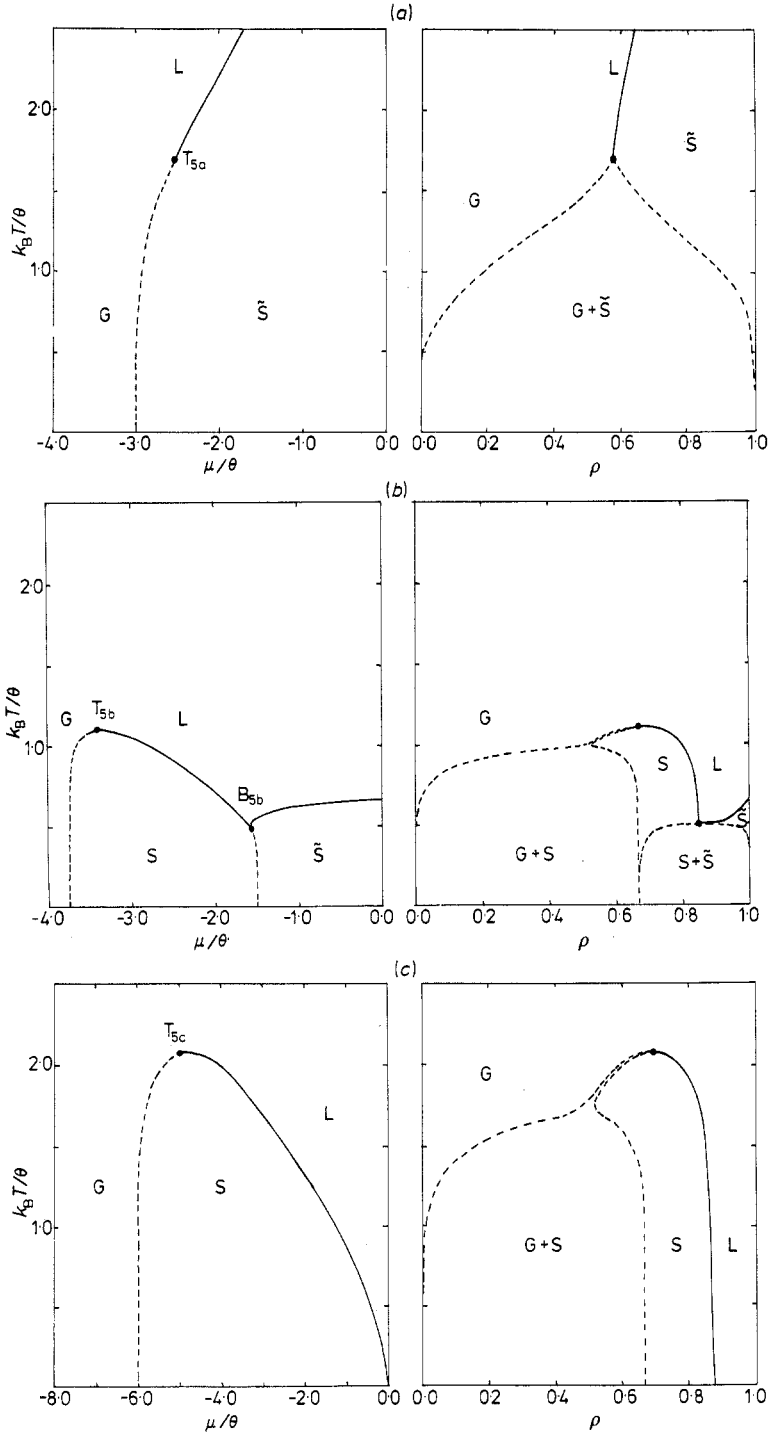

Figure 5. Phase diagrams for $z = +1$ ($\epsilon = 0$) in terms of both the reduced chemical potential μ/θ and the molecular number density ρ. The gas, liquid and close-packed solid phases are denoted by the symbols G, L and $\tilde{S}$ respectively. The open honeycomb solid phase is denoted by S. Regions of coexistence between two phases are indicated with a plus sign between the symbols representing each phase. First-order transitions are indicated by broken curves and second-order transitions are indicated by full curves (*a*) $w/\theta = 0{\cdot}0$, (*b*) $w/\theta = 3{\cdot}5$, (*c*) $w/\theta = 5{\cdot}0$.

subspace. Our investigations indicate that the role played by B^+ is particular to the case $z = +1$ and that for values of z in the range $0 < z < 1$ different fixed points control the transitions. The fact that $z = +1$ represents a special case can be easily seen from the ground-state phase diagram in figure 3(*b*) where for $z = 1$ the point which lies in the extended Potts subspace is also at the coexistence point of the phases C_1, C_2 and C_6. A brief discussion of the more general case is given below in § 3.3.

(ii) $3 < \tilde{w} < 4$. Figure 5(*b*) shows the phase diagram for a typical case with $\tilde{w}$ in this range. Interposed between the gas and close-packed solid phases we now have a region of stability for the open honeycomb solid phase (S) at low temperatures. The transition between the close-packed solid phase ($\tilde{S}$) and the open solid phase (S) as well as the transition between the gas phase (G) and S are first order and described by the fixed points $S\tilde{S}$ and GS respectively. The transitions from the liquid phase to S and $\tilde{S}$ are both second order and controlled by the critical fixed points LS and $L\tilde{S}$ respectively. These two second-order phase boundaries meet at the bicritical point B_{5b} which flows to the bicritical fixed point M of table 2. The first-order gas-open solid phase boundary meets the second-order liquid-open solid boundary at the tricritical point T_{5b} which lies within the domain of attraction of the fixed point AF^+. As the value of $\tilde{w}$ approaches four, the close-packed solid phase $\tilde{S}$ is progressively suppressed.

(iii) $\tilde{w} \geqslant 4$. Figure 5(*c*) shows a typical phase diagram for $\tilde{w} \geqslant 4$ and the behaviour is qualitatively the same as that shown in figure 4(*e*). The various transitions are controlled by the same set of fixed points in both cases.

3.3. $0 < z < 1$

In all of the cases considered for $z = +1$, a first-order liquid–gas transition does not occur. This behaviour is peculiar to $z = +1$ and will be qualitatively different for all positive values of z less than unity. For negative values of z, the appearance of the first-order liquid–gas transition as $\tilde{w}$ increases is marked by the sequence of fixed points N, F, V and this will also be the case for $0 < z < 1$ with F playing the role of a special tricritical fixed point. Hence the phase diagram will be the same as that shown in figure 4(*b*) for values of $\tilde{w}$ in the range $1 + 2z \leqslant \tilde{w} \leqslant 2 + z$. For values of $\tilde{w} > 2 + z$, the open-solid phase has a region of stability between the close-packed solid phase and the gas phase. The appearance of this phase is marked by the sequence of fixed points V, U, Y. The fixed point U is a special critical end-line fixed point which describes the appearance of the second-order transition between the liquid and open-solid phases. The disappearance of the first-order liquid–gas transition at larger values of $\tilde{w}$ is associated with the sequence of fixed points Y, Z, AF^+, just as it is in the case of negative values of z. Hence the case $z = +1$ is special, with the multicritical fixed point B^+ taking us directly from tricritical behaviour described by the fixed point N to tricritical behaviour described by AF^+ without the appearance of a first-order liquid–gas transition.

4. Summary and conclusions

In this paper we have considered a lattice fluid model on a triangular lattice which describes the ordering that may occur in adsorbed monolayers of molecules which have an orientational degree of freedom. The phase diagram was determined for various

choices of the coupling constants using RSRG techniques and the model was found to exhibit many types of complicated multicritical phenomena. The coexistence of both ordered–ordered and ordered–disordered phases occurred. There are four different phases corresponding to the gas, liquid and two distinct types of commensurate solid phase. The fixed points which control the transitions between these different phases were determined and in all the cases studied the melting transition was found to be continuous. Our results may have some application to monolayers of methane or ammonia adsorbed onto a graphite substrate.

Acknowledgments

We wish to acknowledge useful conversations with A Hüller and J W White.

References

Bell G M and Lavis D A 1970 *J. Phys. A: Math. Gen.* **3** 568–81
Berker A N, Ostlund S and Putnam F A 1978 *Phys. Rev.* B **17** 3650–65
Berker A N and Wortis M 1976 *Phys. Rev.* B **14** 4946–63
Blume M 1966 *Phys. Rev.* **141** 517–24
Blume M, Emery V J and Griffiths R B 1971 *Phys. Rev.* A **4** 1071–7
Capel H W 1966 *Physica* **32** 966–88
McTague J P, Nielsen M and Passell L 1979 *Crit. Rev. Solid St. and Mater. Sci.* **7** 135–155
Mahan G D and Girvin S M 1978 *Phys. Rev.* B **17** 4411–5
Niemeijer Th and van Leeuwen J M J 1976 in *Phase Transitions and Critical Phenomena* ed C Domb and M S Green (New York: Academic Press) vol 6 pp 425–505
Nienhuis B and Nauenberg M 1975 *Phys. Rev. Lett.* **35** 477–9
Ostlund S and Berker A N 1979 *Phys. Rev. Lett.* **42** 843–6
Schick M and Griffiths R B 1977 *J. Phys. A: Math. Gen.* **10** 2123–31
Schick M, Walker J S and Wortis M 1977 *Phys. Rev.* B **16** 2205–19
Southern B W and Lavis D A 1980 *J. Phys. A: Math. Gen.* **13**
Thomy A and Duval X 1970 *J. Chim. Phys.* **67** 1101–10
Young A P and Lavis D A 1979 *J. Phys. A: Math. Gen.* **12** 229–43